ЖЭТФ, 2007, том 131, вып. 6, стр. 1048–1063

DZYALOSHINSKY–MORIYA ANTISYMMETRIC EXCHANGE COUPLING IN CUPRATES: OXYGEN EFFECTS

A. S. Moskvin*

Ural State University
620083, Ekaterinburg, Russia

Received October 17, 2006

We reconsider the conventional Moriya approach to the Dzyaloshinsky–Moriya antisymmetric exchange coupling for a single Cu_1–O–Cu_2 bond in cuprates using a perturbation scheme that provides an optimal way to account for intra-atomic electron correlations, the low-symmetry crystal field, and local spin-orbital contributions with a focus on the oxygen term. The Dzyaloshinsky vector and the corresponding weak ferromagnetic moment are shown to be a superposition of comparable and, sometimes, competing local Cu and O contributions. We predict the effect of oxygen staggered spin polarization in the antiferromagnetic edge-shared CuO_2 chains due to the uncompensated oxygen Dzyaloshinsky vectors. The polarization is directed perpendicular to both the main chain antiferromagnetic vector and the CuO_2 chain normal. The intermediate ^{17}O NMR is shown to be an effective tool to inspect the effects of the Dzyaloshinsky–Moriya coupling in an external magnetic field. In particular, we argue that the puzzling planar ^{17}O Knight shift anomalies observed in paramagnetic phase of generic Dzyaloshinsky–Moriya antiferromagnetic cuprate La_2CuO_4 can be assigned to the effect of the field-induced staggered magnetization. Finally, we revisit the effects of symmetric spin anisotropy, in particular, those directly induced by the Dzyaloshinsky–Moriya coupling. The perturbation scheme generalizes the well-known Moriya approach and presents a basis for reliable quantitative estimations of the symmetric partner of the Dzyaloshinsky–Moriya coupling. At variance with the conventional standpoint, the parameters of the effective two-ion spin anisotropy are shown to incorporate the contributions of a single-ion anisotropy for two-hole configurations at both the Cu and O sites.

PACS: 71.70.Ej, 75.30.Et, 75.30.Gw

1. INTRODUCTION

Fifty years ago, Borovik-Romanov and Orlova [1] proposed a spin canting model for weak ferromagnets, whose origin was shortly after [2] related to the exchange-relativistic effect with the mainly antisymmetric exchange coupling. Starting from pioneering papers by Dzyaloshinsky [2] and Moriya [3], the Dzyaloshinsky–Moriya (DM) antisymmetric exchange coupling was extensively investigated in the 1960s–1980s in connection with weak ferromagnetism focusing on hematite α-Fe_2O_3 and orthoferrites $RFeO_3$ [4]. A renewed interest in the subject was motivated by the cuprate problem, in particular, by the weak ferromagnetism observed in La_2CuO_4 [5] and many other interesting effects for the DM systems, in particular, the "field-induced gap" phenomena [6]. At variance with typical three-dimensional systems such as orthoferrites, cuprates are characterized by a low dimensionality, a large diversity of Cu–O–Cu bonds including corner- and edge-sharing, different ladder configurations, strong quantum effects for $s = (1/2)$ Cu^{2+} centers, and a particularly strong Cu–O covalency resulting in a comparable magnitude of hole charge/spin densities at copper and oxygen sites. Several groups (see, e.g., Refs. [7–9]) developed the microscopic model approach by Moriya for different one- and two-dimensional cuprates using different perturbation schemes, different types of the low-symmetry crystalline field, and different approaches to intra-atomic electron–electron repulsion. But despite a rather large number of publications and heated debate (see, e.g., Ref. [10]), the problem of exchange-relativistic effects, that is, of antisymmetric exchange and the related problem of spin anisotropy in cuprates remains open (see, e.g., Refs. [11, 12] for recent exper-

*E-mail: alexandr.moskvin@usu.ru

imental data and discussion). Common shortcomings of current approaches to the DM coupling in $3d$ oxides concern the problem of allocating the Dzyaloshinsky vector and respective "weak" (anti)ferromagnetic moments, and full neglect of spin–orbital effects for "nonmagnetic" O^{2-} ions, which are usually believed to play only an indirect intervening role. On the other hand, the ^{17}O NMR–NQR studies of weak ferromagnet La_2CuO_4 [13] seem to evidence an unconventional local oxygen "weak-ferromagnetic" polarization, whose origin cannot be explained in the framework of current models. All this stimulated a critical reconsideration of many old approaches to the spin–orbital effects in $3d$ oxides, starting from the choice of the proper perturbation scheme and the effective spin Hamiltonian model, usually implying only an indirect intervening role of "nonmagnetic" O^{2-} ions.

In this paper, we revisit the problem of the DM antisymmetric exchange coupling for a single bond in cuprates specifying the local spin–orbital contributions to the Dzyaloshinsky vector and focusing on the oxygen term. In Sec. 2, we present a short overview of the effective spin Hamiltonian of a typical three-center (Cu_1–O–Cu_2) two-hole system. A microscopic theory of the DM coupling is presented in Sec. 3. The Dzyaloshinsky vector is shown to be a superposition of the local Cu and O contributions. In Sec. 4, we examine a response of the DM-coupled Cu_1–O–Cu_2 bond to uniform and staggered external fields, and demonstrate some unusual manifestations of the local oxygen contribution to the DM coupling in edge-sharing CuO_2 chains. In Sec. 5, the intermediate ^{17}O NMR is shown to be an effective tool for inspecting the effects of DM coupling in an external magnetic field. In Sec. 6, we revisit the related problem of symmetric spin anisotropy with the inclusion of local oxygen spin–orbital contributions.

2. SPIN HAMILTONIAN

Below, for illustration, we consider the three-center (Cu_1–O–Cu_2) two-hole system with the tetragonal Cu on-site symmetry and ground Cu $3d_{x^2-y^2}$ states (see Fig. 1), which is typical for cuprates and whose conventional bilinear spin Hamiltonian is written in terms of copper spins as

$$\hat{H}_s(12) = J_{12}(\hat{\mathbf{s}}_1 \cdot \hat{\mathbf{s}}_2) + \mathbf{D}_{12} \cdot [\hat{\mathbf{s}}_1 \times \hat{\mathbf{s}}_2] + \hat{\mathbf{s}}_1 \overleftrightarrow{\mathbf{K}}_{12} \hat{\mathbf{s}}_2, \quad (1)$$

where $J_{12} > 0$ is an exchange integral, $\mathbf{D}_{12}$ is the Dzyaloshinsky vector, and $\overleftrightarrow{\mathbf{K}}_{12}$ is a symmetric second-rank tensor of the anisotropy constants. In contrast with J_{12} and $\overleftrightarrow{\mathbf{K}}_{12}$, the Dzyaloshinsky vector $\mathbf{D}_{12}$ is antisymmetric under site permutation:

$$\mathbf{D}_{12} = -\mathbf{D}_{21}.$$

Hereafter, we write

$$J_{12} = J, \quad \overleftrightarrow{\mathbf{K}}_{12} = \overleftrightarrow{\mathbf{K}}, \quad \mathbf{D}_{12} = \mathbf{D}.$$

We note that using effective spin Hamiltonian (1) implies removing the orbital degree of freedom, which requires caution in the case of the DM coupling because it changes both the spin multiplicity and the orbital state.

It is clear that the applicability of an operator such as $\hat{H}_s(12)$ for describing all the "oxygen" effects is extremely limited. Moreover, the question arises regarding the composite structure and spatial distribution of what is termed the Dzyaloshinsky vector density. This vector is usually assumed to be located at the bond connecting spins 1 and 2.

Strictly speaking, up to a constant, the spin Hamiltonian $\hat{H}_s(12)$ can be viewed as a result of the projection onto the purely ionic ground state

$$Cu_1^{2+}(3d_{x^2-y^2})\text{–}O^{2-}(2p^6)\text{–}Cu_2^{2+}(3d_{x^2-y^2})$$

of the two-hole spin Hamiltonian

$$\hat{H}_s = \sum_{i<j} I(i,j)(\hat{\mathbf{s}}(i)\cdot\hat{\mathbf{s}}(j)) + \sum_{i<j}(\mathbf{d}(i,j)\cdot[\hat{\mathbf{s}}(i)\times\hat{\mathbf{s}}(j)]) + \sum_{i<j} \hat{\mathbf{s}}(i)\overleftrightarrow{\mathbf{K}}(i,j)\,\hat{\mathbf{s}}(j), \quad (2)$$

where the summation ranges holes 1 and 2 rather than sites 1 and 2. This form not only implies both copper and oxygen hole location but also allows accounting for purely oxygen two-hole configurations. Moreover, such a form allows neatly separating the one-center and two-center effects. Two-hole spin Hamiltonian (2) can be projected onto three-center states incorporating the Cu–O charge transfer effects.

For a composite system of two $s = 1/2$ spins, three types of the vector order parameters must be considered,

$$\hat{\mathbf{S}} = \hat{\mathbf{s}}_1 + \hat{\mathbf{s}}_2, \quad \hat{\mathbf{V}} = \hat{\mathbf{s}}_1 - \hat{\mathbf{s}}_2, \quad \hat{\mathbf{T}} = 2[\hat{\mathbf{s}}_1 \times \hat{\mathbf{s}}_2], \quad (3)$$

with the kinematic constraints

$$\begin{aligned} &\hat{\mathbf{S}}^2 + \hat{\mathbf{V}}^2 = 3\hat{\mathbf{I}}, \quad (\hat{\mathbf{S}} \cdot \hat{\mathbf{V}}) = 0, \\ &(\hat{\mathbf{T}} \cdot \hat{\mathbf{V}}) = 6i, \quad [\hat{\mathbf{T}} \times \hat{\mathbf{V}}] = \hat{\mathbf{S}}. \end{aligned} \quad (4)$$

Here, $\hat{\mathbf{S}}$ is the net spin of the pair, the $\hat{\mathbf{V}}$ operator describes the effect of local antiferromagnetic order, or

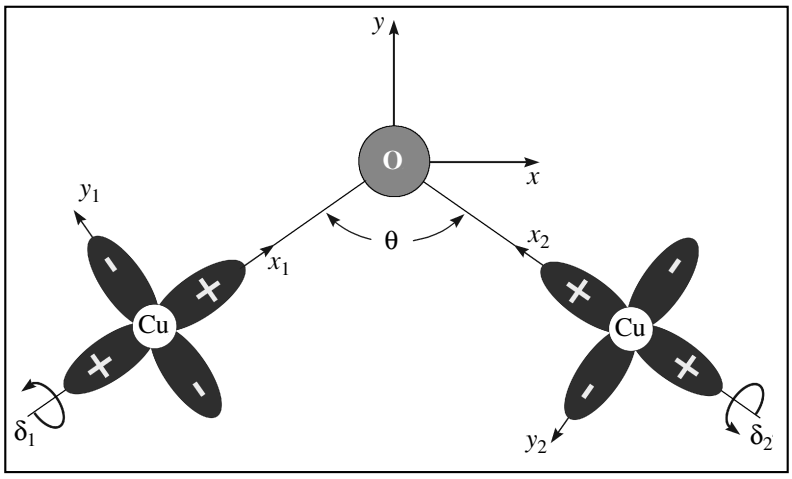

Fig. 1. Geometry of the three-center (Cu–O–Cu) two-hole system with ground Cu $3d_{x^2-y^2}$ states

staggered spin polarization, and the $\hat{\mathbf{T}}$ operator can be associated with the vector chirality [14]. In recent years, phases with the broken vector chirality in frustrated quantum spin chains have attracted considerable interest. Such phases are characterized by nonzero long-range correlations of the vector order parameter $\langle\hat{\mathbf{T}}\rangle$. Interestingly, a chirally ordered phase can manifest itself as a "nonmagnetic" one, with

$$\langle\hat{\mathbf{S}}\rangle = \langle\hat{\mathbf{V}}\rangle = 0.$$

Both $\hat{\mathbf{T}}$ and $\hat{\mathbf{V}}$ operators change the net spin multiplicity with the matrix elements

$$\langle 00|\hat{T}_m|1n\rangle = -\langle 1n|\hat{T}_m|00\rangle = i\delta_{mn},$$

$$\langle 00|\hat{V}_m|1n\rangle = \langle 1n|\hat{V}_m|00\rangle = \delta_{mn}, \qquad (5)$$

where we use a Cartesian basis for $S = 1$. The eigenstates of the operators $\hat{V}_n$ and $\hat{T}_n$ with the nonzero eigenvalues ± 1 form Néel doublets

$$\frac{1}{\sqrt{2}}(|00\rangle \pm |1n\rangle)$$

and Dzyaloshinsky–Moriya doublets

$$\frac{1}{\sqrt{2}}(|00\rangle \pm i|1n\rangle),$$

respectively. The Néel doublets correspond to classical collinear antiferromagnetic spin configurations and the Dzyaloshinsky–Moriya doublets correspond to quantum spin configurations that are sometimes associated with a rectangular 90° spin ordering in the plane orthogonal to the Dzyaloshinsky vector.

We note that both the above spin Hamiltonians can be reduced up to a constant to the spin operator

$$\hat{H}_S = \frac{1}{4}J(\hat{\mathbf{S}}^2 - \hat{\mathbf{V}}^2) + \frac{1}{2}(\mathbf{D}\cdot\hat{\mathbf{T}}) + \\ + \frac{1}{4}\hat{\mathbf{S}}\overleftrightarrow{\mathbf{K}}^{S}\hat{\mathbf{S}} - \frac{1}{4}\hat{\mathbf{V}}\overleftrightarrow{\mathbf{K}}^{V}\hat{\mathbf{V}} \qquad (6)$$

acting in a net spin space. For simple dipole-like two-ion anisotropy as in Eq. (1),

$$\overleftrightarrow{\mathbf{K}}^{S} = \overleftrightarrow{\mathbf{K}}^{V} = \overleftrightarrow{\mathbf{K}},$$

although these tensorial parameters can differ from each other in general. Using the anticommutator relations

$$\{\hat{S}_i, \hat{S}_j\} + \{\hat{V}_i, \hat{V}_j\} = 2\delta_{ij}, \quad \{\hat{V}_i, \hat{V}_j\} = \{\hat{T}_i, \hat{T}_j\}, \qquad (7)$$

we conclude that the effective operator of symmetric anisotropy can be equivalently expressed in terms of the symmetric products $\{\hat{S}_i, \hat{S}_j\}$, $\{\hat{V}_i, \hat{V}_j\}$, or $\{\hat{T}_i, \hat{T}_j\}$.

The most general form of spin Hamiltonian (6) does not discriminate between copper or oxygen contribution and can be used to properly account for oxygen effects. As we see below, the $\mathbf{D}$ and $\overleftrightarrow{\mathbf{K}}$ parameters allow the correct separation of local copper and oxygen contributions.

Generally speaking, expressions (1), (2), and (6) represent the effective Hamiltonians that are not strictly equivalent to each other. Indeed, the basic form (1) implies only the two-ion pseudodipole contribution to the anisotropy parameters $\overleftrightarrow{\mathbf{K}}_{12}$, while Hamiltonians (2) and (6) allow for the single-ion anisotropy for the two-hole oxygen configuration (see below). The

effective use of either form strongly depends on the perturbation scheme applied. Below, we use form (6), which is most efficient in describing the exchange-relativistic effects. We note that the net spin representation and the quantum approach in general are especially efficient in describing antisymmetric exchange in Cu–Cu dimer systems (see, e.g., Ref. [15] and the references therein). The classical approach to the $s = 1/2$ spin Hamiltonian should be applied with caution, particularly for one-dimensional systems.

Before proceeding with the microscopic analysis, we note that the interaction of our three-center system with external spins and/or fields $\hat{H}_{ext}$ is usually addressed by introducing only two types of effective external fields: the conventional Zeeman-like uniform field and an unconventional Néel-like staggered field, such that $\hat{H}_{ext}$ is given by

$$\hat{H}_{ext} = -(\mathbf{h}^S \cdot \hat{\mathbf{S}}) - (\mathbf{h}^V \cdot \hat{\mathbf{V}}). \tag{8}$$

We note that an ideal Néel state is attainable only in the limit of the infinitely large staggered field, and therefore, for a finite staggered field $\mathbf{h}^V \parallel \mathbf{n}$, the ground state is a superposition of a spin singlet and a Néel state,

$$\Psi = \cos\alpha|00\rangle + \sin\alpha|1n\rangle, \quad \operatorname{tg} 2\alpha = \frac{2h^V}{J},$$

whose composition reflects the role of quantum effects. For instance, in a Heisenberg spin-1/2 chain with nn exchange, the maximum value of the staggered field is $h^V = J/2$, and hence the Ψ function strongly differs from that of the Néel state,

$$\langle \hat{V}_n \rangle = \sin 2\alpha = \frac{1}{\sqrt{2}},$$

and the quantum mechanical average for a single spin

$$\langle s_z \rangle \le \frac{1}{2}\sin\frac{\pi}{4} = \frac{1}{\sqrt{2}} \cdot \frac{1}{2} \approx 0.71 \cdot \frac{1}{2}$$

deviates strongly from the classical value 1/2. We note that for an isolated antiferromagnetically coupled spin pair, the zero-temperature uniform spin susceptibility vanishes:

$$\chi^S = 0,$$

while for the staggered spin susceptibility, we obtain

$$\chi^V = 2/J.$$

3. MICROSCOPIC THEORY OF THE DZYALOSHINSKY–MORIYA COUPLING IN CUPRATES

3.1. Preliminaries

To derive the microscopic expression for the Dzyaloshinsky vector, Moriya [3] used Anderson's formalism of superexchange interaction [16] with two main contributions of the so-called kinetic and potential exchange. Then he took the spin-orbital corrections to the effective d–d transfer integral and potential exchange into account. Such an approach seems to be inappropriate to account for purely oxygen effects. In subsequent papers (see, e.g., Refs. [8, 17]), the authors used the Moriya scheme to account for spin–orbital corrections to the p–d transfer integral, but without any analysis of the oxygen contribution. It is worth noting that in both instances, the spin–orbital renormalization of a single-hole transfer integral leads immediately to many problems with the correct responsiveness of the on-site Coulomb hole–hole correlation effects. Anyway, the effective DM spin Hamiltonian evolves from the higher-order perturbation effects, which makes its analysis rather involved and leads to many misleading conclusions.

At variance with the Moriya approach, we start with the construction of spin-singlet and spin-triplet wave functions for our three-center two-hole system taking account of the p–d hopping, on-site hole–hole repulsion, and crystal field effects for excited configurations $\{n\}$ (011, 110, 020, 200, 002) with different hole occupation of Cu_1, O, and Cu_2 sites, respectively. The p–d hopping for a Cu–O bond implies the conventional Hamiltonian

$$\hat{H}_{pd} = \sum_{\alpha,\beta} t_{p\alpha d\beta} \hat{p}^\dagger_\alpha \hat{d}_\beta + \text{h.c.}, \tag{9}$$

where $\hat{p}^\dagger_\alpha$ creates a hole in the α state at the oxygen site, and $\hat{d}_\beta$ annihilates a hole in the β state at the copper site; $t_{p\alpha d\beta}$ is the p–d transfer integral,

$$t_{p_x d_{x^2-y^2}} = \frac{\sqrt{3}}{2} t_{p_z d_{z^2}} = t_{pd\sigma} > 0, t_{p_y d_{xy}} = t_{pd\pi} > 0.$$

For the basic 101 configuration with two $d_{x^2-y^2}$ holes localized at their parent sites, we obtain the perturbed wave function

$$\Psi_{101;SM} = \Phi_{101;SM} + \\ + \sum_{\{n\},\Gamma} c_{\{n\}}({}^{2S+1}\Gamma)\Phi_{\{n\};\Gamma SM}, \tag{10}$$

where the summation ranges both different configurations and different orbital Γ states. It is worth noting that the probability amplitudes

$$c_{\{011\}}, c_{\{110\}} \propto t_{pd}, \quad c_{\{200\}}, c_{\{020\}}, c_{\{002\}} \propto t^2_{pd}.$$

To account for orbital effects for $Cu_{1,2}$ $3d$ holes and the covalency-induced mixing of different orbital states for the 101 configuration, we introduce an effective exchange Hamiltonian

$$\hat{H}_{ex} = \\ = \frac{1}{2}\sum_{\alpha\beta\gamma\delta\mu\mu'} J(\alpha\beta\gamma\delta)\hat{d}^{\dagger}_{1\alpha\mu}\hat{d}^{\dagger}_{2\beta\mu'}\hat{d}_{2\gamma\mu}\hat{d}_{1\delta\mu'} + \text{h.c.}, \quad (11)$$

where $\hat{d}^{\dagger}_{1\alpha\mu}$ creates a hole in the αth $3d$ orbital at a Cu_1 site with the spin projection μ. Exchange Hamiltonian (11) involves both spinless and spin-dependent terms, but it preserves the spin multiplicity of the Cu_1–O–Cu_2 system. The exchange parameters $J(\alpha\beta\gamma\delta)$ are of the order of t^4_{pd}.

We next introduce the standard effective spin Hamiltonian acting in a four-fold spin-degenerate space of the basic 101 configuration with two $d_{x^2-y^2}$ holes. We then easily calculate the singlet–triplet separation to find the effective exchange integral

$$J_{12} = J(d_{x^2-y^2}d_{x^2-y^2}d_{x^2-y^2}d_{x^2-y^2}),$$

and calculate the singlet–triplet mixing due to three local spin-orbital terms $V_{so}(Cu_1)$, $V_{so}(O)$, and $V_{so}(Cu_2)$ to find the local contributions to Dzyaloshinsky vector:

$$\mathbf{D} = \mathbf{D}^{(1)} + \mathbf{D}^{(O)} + \mathbf{D}^{(2)}. \quad (12)$$

The local spin–orbital coupling is taken in the form

$$V_{so} = \sum_i \xi_{nl}(\mathbf{l}_i \cdot \mathbf{s}_i) = \frac{\xi_{nl}}{2} \times \\ \times [(\hat{\mathbf{l}}_1+\hat{\mathbf{l}}_2)\cdot\hat{\mathbf{S}}+(\hat{\mathbf{l}}_1-\hat{\mathbf{l}}_2)\cdot\hat{\mathbf{V}}] = \hat{\mathbf{\Lambda}}^S\cdot\hat{\mathbf{S}}+\hat{\mathbf{\Lambda}}^V\cdot\hat{\mathbf{V}} \quad (13)$$

with a single-particle constant $\xi_{nl} > 0$ for electrons and $\xi_{nl} < 0$ for holes. We use the orbital matrix elements

$$\langle d_{x^2-y^2}|l_x|d_{yz}\rangle = \langle d_{x^2-y^2}|l_y|d_{xz}\rangle = i,$$

$$\langle d_{x^2-y^2}|l_z|d_{xy}\rangle = -2i, \quad \langle i|l_j|k\rangle = -i\epsilon_{ijk}$$

with Cu $3d_{yz}$=$|1\rangle$, $3d_{xz}$=$|2\rangle$, $3d_{xy}$=$|3\rangle$ for Cu $3d$ holes, and

$$\langle p_i|l_j|p_k\rangle = i\epsilon_{ijk}$$

for O $2p$ holes. A free cuprous Cu^{2+} ion is described by a large spin–orbital coupling with $|\xi_{3d}| \approx 0.1$ eV (see, e.g., Ref. [18]), although its value may be significantly reduced in oxides. Information regarding the ξ_{2p} value for the O^{2-} ion in oxides is scant, if any. The spin–orbital coupling on oxygen is usually taken to be much smaller than that on copper, and is therefore neglected [19, 20]. But even for a free oxygen atom, the electron spin–orbital coupling turns out to reach an appreciable magnitude: $\xi_{2p} \approx 0.02$ eV [21], while for the O^{2-} ion in oxides, a visible enhancement of the spin–orbital coupling is expected because the $2p$ wave function is more compact [22]. If we account for $\xi_{nl} \propto \langle r^{-3}\rangle_{nl}$ and compare these quantities for copper ($\langle r^{-3}\rangle_{3d} \approx 6$–$8$ a.u. [22]) and oxygen ($\langle r^{-3}\rangle_{2p} \approx 4$ a.u. [13, 22]), we obtain the difference between ξ_{3d} and ξ_{2p} by at least a factor of two.

Hereafter, we assume a tetragonal symmetry at Cu sites with local coordinate systems as shown in Fig. 1. The global xyz coordinate system is chosen such that the Cu_1–O–Cu_2 plane coincides with the xy plane and the x axis is directed along the Cu_1–Cu_2 bond (see Fig. 1). The basic unit vectors $\mathbf{x}$, $\mathbf{y}$, and $\mathbf{z}$ can then be written in local systems of Cu_1 and Cu_2 sites as

$$\mathbf{x} = (\sin\frac{\theta}{2}, -\cos\frac{\theta}{2}\cos\delta_1, -\cos\frac{\theta}{2}\sin\delta_1),$$

$$\mathbf{y} = \left(\cos\frac{\theta}{2}, \sin\frac{\theta}{2}\cos\delta_1, \sin\frac{\theta}{2}\sin\delta_1\right),$$

$$\mathbf{z} = (0, \sin\delta_1, \cos\delta_1)$$

for Cu_1, with θ, δ_1 to be replaced by $-\theta, \delta_2$ for Cu_2. The exchange integral can be written as

$$J = \sum_{\{n\},\Gamma} [|c_{\{n\}}(^3\Gamma)|^2 E_{^3\Gamma}(\{n\}) - \\ - |c_{\{n\}}(^1\Gamma)|^2 E_{^1\Gamma}(\{n\})]. \quad (14)$$

As regards the DM interaction, we deal with two competing contributions. The first is derived as a first-order contribution, which does not take $Cu_{1,2}$ $3d$-orbital fluctuations for the ground state 101 configuration into account. Projecting spin–orbital coupling (13) onto states (10), we see that the $\hat{\mathbf{\Lambda}}^V\cdot\hat{\mathbf{V}}$ term is equivalent to the purely spin DM coupling with local contributions to the Dzyaloshinsky vector

$$D^{(m)}_i = -2i\langle 00|V_{so}(m)|1i\rangle = \\ = -2i\sum_{\{n\},\Gamma_1,\Gamma_2} c^*_{\{n\}}(^1\Gamma_1)c_{\{n\}}(^3\Gamma_2) \times \\ \times \langle\Phi_{\{n\};\Gamma_1 00}|\Lambda^V_i|\Phi_{\{n\};\Gamma_2 1i}\rangle. \quad (15)$$

In all the instances, the nonzero contribution to the local Dzyaloshinsky vector is determined solely by the spin–orbital singlet–triplet mixing for the one-site 200, 020, 002 and two-site 110, 011 two-hole configurations, respectively. For one-site two-hole configurations, we have

$$\mathbf{D}^{(200)} = \mathbf{D}^{(1)}, \quad \mathbf{D}^{(020)} = \mathbf{D}^{(O)}, \quad \mathbf{D}^{(002)} = \mathbf{D}^{(2)}.$$

The second contribution, associated with $Cu_{1,2}$ 3d-orbital fluctuations within a ground state 101 configuration, is more familiar; it evolves from a second-order combined effect of $Cu_{1,2}$ spin–orbital $V_{so}(Cu_{1,2})$ and the effective orbitally anisotropic Cu_1–Cu_2 exchange coupling

$$D_i^{(m)} = -2i\langle 00|V_{so}(m)|1i\rangle = -2i\sum_{\Gamma}\frac{\langle\{101\};\Gamma_s 00|\hat{\Lambda}_i^V|\{101\};\Gamma 1i\rangle\langle\{101\};\Gamma 1i|\hat{H}_{ex}|\{101\};\Gamma_t 1i\rangle}{E_{^3\Gamma_t}(\{101\}) - E_{^3\Gamma}(\{101\})} -$$

$$- 2i\sum_{\Gamma}\frac{\langle\{101\};\Gamma_s 00|\hat{H}_{ex}|\{101\};\Gamma 00\rangle\langle\{101\};\Gamma 00|\hat{\Lambda}_i^V|\{101\};\Gamma_t 1i\rangle}{E_{^1\Gamma_s}(\{101\}) - E_{^1\Gamma}(\{101\})}. \quad (16)$$

We note that at variance with the original Moriya approach [3], both spinless and spin-dependent parts of the exchange Hamiltonian contribute additively and comparably to the DM coupling, because of the same magnitude and opposite sign of the singlet–singlet and triplet–triplet exchange matrix elements on the one hand and the orbital antisymmetry of spin–orbital matrix elements on the other hand.

It is easy to see that the contributions of 002 and 200 configurations to the Dzyaloshinsky vector bear a similarity to the respective second type ($\propto V_{so}H_{ex}$) contributions; however, in the former we deal with the spin–orbital coupling for two-hole $Cu_{1,2}$ configurations, while in the latter, with that of one-hole $Cu_{1,2}$ configurations.

3.2. Copper contribution

We first address a relatively simple instance of a strong rhombic crystal field for intermediate oxygen ion with the crystal field axes oriented along global coordinate x, y, z axes. It is worth noting that in such a case, the O $2p_z$ orbital does not play an active role in either symmetric or antisymmetric (DM) exchange interaction and that the Cu $3d_{yz}$ orbital appears to be inactive in the DM interaction due to a zero overlap/transfer with O $2p$ orbitals.

For illustration, we consider the first contribution (15) of the one-site 200, 002 two-hole configurations $d^2_{x^2-y^2}$, $d_{x^2-y^2}d_{xy}$, and $d_{x^2-y^2}d_{xz}$, which do covalently mix with the ground state configuration. Calculating the singlet–triplet mixing matrix elements in the global coordinate system, we find all the components of the local Dzyaloshinsky vectors. The Cu_1 contribution turns out to be nonzero only for the 200 configuration, and can be written as a sum of several terms. We first give the contribution of the singlet $(d^2_{x^2-y^2})^1A_{1g}$ state:

$$\begin{aligned}
&D_x^{(1)} = -2i\langle 00|V_{so}(\mathrm{Cu}_1)|1x\rangle = \\
&= \sqrt{2}\xi_{3d}\, c_{200}({}^1A_{1g}) \times \\
&\times [c_{200}({}^3E_g)\cos\delta_1 - 2c_{200}({}^3A_{2g})\sin\delta_1]\cos\frac{\theta}{2}, \\
&D_y^{(1)} = -2i\langle 00|V_{so}(\mathrm{Cu}_1)|1y\rangle = \\
&= -\sqrt{2}\xi_{3d}\, c_{200}({}^1A_{1g}) \times \\
&\times [c_{200}({}^3E_g)\cos\delta_1 - 2c_{200}({}^3A_{2g})\sin\delta_1]\sin\frac{\theta}{2}, \\
&D_z^{(1)} = -2i\langle 00|V_{so}(\mathrm{Cu}_1)|1z\rangle = \\
&= -\sqrt{2}\xi_{3d}\, c_{200}({}^1A_{1g}) \times \\
&\times [c_{200}({}^3E_g)\sin\delta_1 - 2c_{200}({}^3A_{2g})\cos\delta_1],
\end{aligned} \quad (17)$$

where

$$c_{200}({}^1A_{1g}) = -\frac{3}{2\sqrt{2}}t^2_{pd\sigma}\frac{1}{E_{^1A_{1g}}}\left[\frac{\sin^2\dfrac{\theta}{2}}{\epsilon_x} - \frac{\cos^2\dfrac{\theta}{2}}{\epsilon_y}\right],$$

$$c_{200}({}^{1,3}A_{2g}) = -\frac{\sqrt{3}}{4}t_{pd\sigma}t_{pd\pi}\frac{1}{E_{^{1,3}A_{2g}}} \times \left(\frac{1}{\epsilon_x} + \frac{1}{\epsilon_y}\right)\sin\theta\cos\delta_1,$$

$$c_{200}({}^{1,3}E_g) = -\frac{\sqrt{3}}{4}t_{pd\sigma}t_{pd\pi}\frac{1}{E_{^{1,3}E_g}} \times \left(\frac{1}{\epsilon_x} + \frac{1}{\epsilon_y}\right)\sin\theta\sin\delta_1$$

are the respective probability amplitudes for the singlet $(d^2_{x^2-y^2})^1A_{1g}$ and the singlet/triplet $(d_{x^2-y^2}d_{xy})^{1,3}A_{2g}$, $(d_{x^2-y^2}d_{xz})^{1,3}E_g$ 200 configurations in the ground state wave function. Here,

$$E_{^1A_{1g}} = A + 4B + 3C$$

is the energy of the two-hole copper singlet with the $d^2_{x^2-y^2}$ configuration and

$$E_{^1A_{2g}} = \epsilon_{xy} + A + 4B + 2C,$$

$$E_{^3A_{2g}} = \epsilon_{xy} + A + 4B,$$

$$E_{^1E_g} = \epsilon_{xz} + A + B + 2C,$$

$$E_{^3E_g} = \epsilon_{xz} + A - 5B$$

are the energies of the two-hole copper terms with $d_{x^2-y^2}d_{xy}$ and $d_{x^2-y^2}d_{xz}$ configurations, with A, B, and C being the Racah parameters. Taking into account that[1)]

$$c_{002}(^1A_{1g}) = c_{200}(^1A_{1g}), \quad c_{002}(^3A_{2g}) = c_{200}(^3A_{2g}),$$

$$c_{002}(^3E_{2g}) = c_{200}(^3E_g),$$

we see that the Cu_2 contribution to the Dzyaloshinsky vector can be obtained from Eqs. (17) if θ, δ_1 are replaced by $-\theta, \delta_2$. Interestingly,

$$D_{x,y}^{(1,2)} \propto \sin\theta \, \sin 2\delta_{1,2}.$$

Both collinear ($\theta = \pi$) and rectangular ($\theta = \pi/2$) superexchange geometries appear to be unfavorable for copper contribution to the antisymmetric exchange, although the result in the rectangular geometry strongly depends on the relation between the energies of O $2p_x$ and $2p_y$ orbitals. Contributions of the singlet $(d_{x^2-y^2}d_{xy})^1A_{2g}$ and $(d_{x^2-y^2}d_{xz})^1E_g$ states to the Dzyaloshinsky vector are

$$d_x^{(1)} = d^{(1)} \sin\frac{\theta}{2}, \quad d_y^{(1)} = d^{(1)} \cos\frac{\theta}{2}, \quad d_z^{(1)} = 0,$$

where

$$d^{(1)} = \xi_{3d}(c_{200}(^1A_{2g})c_{200}(^3E_g) - c_{200}(^1E_g)c_{200}(^3A_{2g})).$$

Here, we deal with a vector directed along the Cu_1–O bond, whose modulus

$$d^{(1)} \propto \sin^2\theta \sin 2\delta_1$$

is determined by partial cancellation of two terms.

It is easy to see that the copper $V_{so}(1)$ contribution to the Dzyaloshinsky vector for two-site 110 and 011 configurations is determined by the d–p-exchange.

3.3. Oxygen contribution

With the same assumption regarding the orientation of the rhombic crystal field axes for the intermediate oxygen ion, the local oxygen contribution to the Dzyaloshinsky vector for the one-site 020 configuration turns out to be oriented along the local O_z axis and can be written as

$$D_z^{(0)} = -2i\langle 00|V_{so}(\mathrm{O})|1z\rangle = \\ = \sqrt{2}\xi_{2p}\, c_t(p_xp_y)[c(p_x^2) + c(p_y^2)], \quad (18)$$

where

$$c(p^2) = c_{020}(p^2),$$

$$c(p_x^2) = -\frac{3}{2\sqrt{2}}t_{pd\sigma}^2 \frac{\sin^2\frac{\theta}{2}}{\epsilon_x E_s(p_x^2)},$$

$$c(p_y^2) = \frac{3}{2\sqrt{2}}t_{pd\sigma}^2 \frac{\cos^2\frac{\theta}{2}}{\epsilon_y E_s(p_y^2)},$$

$$c_t(p_xp_y) = \frac{3}{8}t_{pd\sigma}^2\left(\frac{1}{\epsilon_x} + \frac{1}{\epsilon_y}\right)\frac{\sin\theta}{E_t(p_xp_y)} \quad (19)$$

are the respective probability amplitudes for the singlet, p_x^2, p_y^2, and triplet p_xp_y 020 configurations in the ground state wave function;

$$E_s(p_{x,y}^2) = 2\epsilon_{x,y} + F_0 + \frac{4}{25}F_2,$$

$$E_t(p_xp_y) = \epsilon_x + \epsilon_y + F_0 - \frac{1}{5}F_2$$

are the energies of the oxygen two-hole singlet (s) and triplet (t) configurations p_x^2, p_y^2 and p_xp_y, respectively, and F_0 and F_2 are Slater integrals. This vector can be written as[2)]

$$\mathbf{D}^{(\mathrm{O})} = D_{\mathrm{O}}(\theta)[\mathbf{r}_1 \times \mathbf{r}_2], \quad (20)$$

where $\mathbf{r}_{1,2}$ are unit radius vectors along $Cu_{1,2}$–O bonds, and

$$D_{\mathrm{O}}(\theta) = \frac{9\xi_{2p}t_{pd\sigma}^4}{16}\frac{1}{E_t(p_xp_y)}\left(\frac{1}{\epsilon_x} + \frac{1}{\epsilon_y}\right) \times \\ \times \left[\frac{\cos^2\frac{\theta}{2}}{\epsilon_x E_s(p_x^2)} - \frac{\sin^2\frac{\theta}{2}}{\epsilon_y E_s(p_y^2)}\right]. \quad (21)$$

It is worth noting that $\mathbf{D}^{(\mathrm{O})}$ is independent of the δ_1 and δ_2 angles. The $D_{\mathrm{O}}(\theta)$ dependence is expected to be rather smooth without any singularities for collinear and rectangular superexchange geometries.

[1)] This is true up to the replacement $\delta_1 \leftrightarrow \delta_2$. We note that the probability amplitudes for triplet 200 and 002 configurations are of the same sign due to the double-minus effect: 1) the $\theta \leftrightarrow -\theta$ replacement and 2) the antisymmetry of orbital functions: the 200-function $\propto d_{x^2-y^2}(1)d_{xy}(2)$, while the 002-function $\propto d_{x^2-y^2}(2)d_{xy}(1)$.

[2)] Such a simple and helpful formula for the Dzyaloshinsky vector was phenomenologically proposed in Ref. [23] and microscopically derived by Moskvin (see, e.g., Ref. [4]).

The local oxygen contribution to the Dzyaloshinsky vector for two-site 110 and 011 configurations is also oriented along the local O_z axis and can be written as

$$D_z^{(O)} = -2i\langle 00|V_{so}(O)|1z\rangle = \\ = \xi([\mathbf{c}_s(dp)\times\mathbf{c}_t(dp)]_z + [\mathbf{c}_s(pd)\times\mathbf{c}_t(pd)]_z), \quad (22)$$

$$c_{s,t}(dp_x) = -\frac{\sqrt{3}}{2}\,\frac{t_{pd\sigma}}{E_{s,t}(dp_x)}\sin\frac{\theta}{2}, \\ c_{s,t}(dp_y) = -\frac{\sqrt{3}}{2}\,\frac{t_{pd\sigma}}{E_{s,t}(dp_y)}\cos\frac{\theta}{2}, \quad (23)$$

where

$$c_{s,t}(dp) = c_{110}(dp), \quad c_{s,t}(pd) = c_{011}(dp)$$

are the respective probability amplitudes for different singlet (c_s) and triplet (c_t) 110 ($d_{x^2-y^2}p_{x,y}$) and 011 ($p_{x,y}d_{x^2-y^2}$) configurations in the ground state wave function. The energies $E_{s,t}(dp_{x,y})$ are those for singlet and triplet states of $dp_{x,y}$ configurations:

$$E_{s,t}(dp_{x,y}) = \epsilon_{x,y} + K_{dpx,y} \pm I_{dpx,y},$$

where $K_{dpx,y}$ and $I_{dpx,y}$ are Coulomb and d–p-exchange integrals, respectively. It is easy to see that the nonzero contribution to the Dzyaloshinsky vector is determined by a direct d–p-exchange and can be written similarly to (20) with

$$D_O(\theta) = \frac{3\xi_{2p}t_{pd\sigma}^2}{8}\,\frac{1}{\epsilon_x\epsilon_y}\left(\frac{I_{dpx}}{\epsilon_x} - \frac{I_{dpy}}{\epsilon_y}\right) \approx \\ \approx \frac{3\xi_{2p}t_{pd\sigma}^2}{8}\,\frac{1}{\epsilon_x\epsilon_y}\left(\frac{\sin^2\frac{\theta}{2}}{\epsilon_x} - \frac{\cos^2\frac{\theta}{2}}{\epsilon_y}\right) I_{dp\sigma}, \quad (24)$$

where we take only the d–p–σ-exchange into account ($I_{dp\sigma} \propto t_{pd\sigma}^2$).

3.4. Comment on microscopic estimations of Dzyaloshinsky vectors

Thus, the net Dzyaloshinsky vector **D** is a superposition of three contributions (see (12)) associated with the respective sites. In general, all the vectors can be oriented differently. Comparative analysis of Eqs. (17), (21), and (24) with the estimates for different parameters typical for cuprates given in [24] ($t_{pd\sigma} \approx 1.5$ eV, $t_{pd\pi} \approx 0.7$ eV, $A = 6.5$ eV, $B = 0.15$ eV, $C = 0.58$ eV, $F_0 = 5$ eV, and $F_2 = 6$ eV) evidences that copper and oxygen Dzyaloshinsky vectors can be of comparable magnitude. However, this in fact strongly depends on the Cu_1–O–Cu_2 bond geometry and crystal field effects. The latter determines the single-hole energies for both O $2p$- and Cu $3d$-holes such as $\epsilon_{x,y}$ and $\epsilon_{xy,xz}$, whose values are usually of the order of 1 eV and 1–3 eV [25], respectively. It is worth noting that for two limiting bond geometries, $\theta \sim \pi$ and $\theta \sim \pi/2$ (nearly collinearly and nearly rectangular bonding), we deal with a strong "geometry reduction" of the DM coupling due to the $\sin\theta$ factor for the first geometry and the factor

$$\left[\frac{\sin^2\frac{\theta}{2}}{\epsilon_x} - \frac{\cos^2\frac{\theta}{2}}{\epsilon_y}\right]$$

for the second. Indeed, the resulting effect for the nearly rectangular Cu_1–O–Cu_2 bonding appears to be very sensitive to the local oxygen crystal field. A critical angle θ_{Cu} at which the Cu contribution to the Dzyaloshinsky vector vanishes is defined as

$$\mathrm{tg}^2\,\frac{\theta_{Cu}}{2} = \frac{\epsilon_x}{\epsilon_y}$$

For the oxygen contribution in (21), we arrive at another critical angle:

$$\mathrm{tg}^2\,\frac{\theta_O}{2} = \frac{\epsilon_y E_s(p_y^2)}{\epsilon_x E_s(p_x^2)}.$$

The maximum value of the scalar parameter $D_O(\theta)$ that determines the oxygen contribution to the Dzyaloshinsky vector can be estimated to be of the order of 1 meV for the typical parameters mentioned above. As a whole, our model microscopic theory is believed to provide a reasonable estimation of the direction and numerical value of the Dzyaloshinsky vectors. A seemingly more important result concerns the elucidation of the role played by the Cu_1–O–Cu_2 bond geometry, crystal field, and correlation effects.

3.5. Dzyaloshinsky–Moriya coupling in La_2CuO_4

The DM coupling and magnetic anisotropy in La_2CuO_4 and related compounds have attracted considerable attention in the 1990s (see, e.g., Refs. [7–9]), and are still debated in the literature [11, 12]. In the low-temperature tetragonal (LTT) and orthorhombic (LTO) phases of La_2CuO_4, the oxygen octahedra surrounding each copper ion rotate by a small tilting angle ($\delta_{LTT} \approx 3^\circ$, $\delta_{LTO} \approx 5^\circ$) relative to their location in the high-temperature tetragonal phase. The structural distortion allows the appearance of the antisymmetric DM coupling. For the LTT phase, in terms of our choice

of structural parameters to describe the Cu_1–O–Cu_2 bond, we have

$$\theta = \pi, \quad \delta_1 = \delta_2 = \frac{\pi}{2} \pm \delta_{LTT}$$

for bonds oriented perpendicular to the tilting plane, and

$$\theta = \pm(\pi - 2\delta_{LTT}), \quad \delta_1 = \delta_2 = \frac{\pi}{2}$$

for bonds oriented parallel to the tilting plane. This means that all the local Dzyaloshinsky vectors vanish for the former bonds, and are orthogonal to the tilting plane for the latter bonds. For the LTO phase,

$$\theta = \pm(\pi - \sqrt{2}\delta_{LTO}), \quad \delta_1 = \delta_2 = \frac{\pi}{2} \pm \delta_{LTO}.$$

In this case, the largest ($\propto \delta_{LTO}$) component of the local Dzyaloshinsky vectors (z-component in our notation) is oriented perpendicular to the Cu_1–O–Cu_2 bond plane. The other two components of the local Dzyaloshinsky vectors are fairly small: the one perpendicular to the CuO_2 plane (y-component in our notation) is of the order of δ^2_{LTO}, and the one oriented along the Cu_1–Cu_2 bond axis (x-component in our notation) is of the order of δ^3_{LTO}.

4. DZYALOSHINSKY–MORIYA COUPLED Cu_1–O–Cu_2 BOND IN EXTERNAL FIELDS

4.1. Uniform external magnetic field

Application of a uniform external magnetic field $\mathbf{h}_S$ produces a staggered spin polarization in the antiferromagnetically coupled Cu_1–Cu_2 pair,

$$\langle \mathbf{V}_{12} \rangle = \mathbf{L} = -\frac{1}{J^2_{12}} \left[\sum_i \mathbf{D}^{(i)}_{12} \times \mathbf{h}^S \right] = \overleftrightarrow{\chi}^{VS} \mathbf{h}^S \quad (25)$$

with an antisymmetric VS-susceptibility tensor:

$$\chi^{VS}_{\alpha\beta} = -\chi^{VS}_{\beta\alpha}.$$

We see that the direction of the staggered spin polarization, or antiferromagnetic vector, depends on that of the Dzyaloshinsky vector [26]. The VS coupling results in many interesting effects for the DM systems, in particular, the "field-induced gap" phenomena in one-dimensional $s = 1/2$ antiferromagnetic Heisenberg system with alternating DM coupling [6]. Approximately, the phenomenon is described by the so-called staggered $s = 1/2$ antiferromagnetic Heisenberg model with the Hamiltonian

$$\hat{H} = J \sum_i (\hat{\mathbf{s}}_i \cdot \hat{\mathbf{s}}_{i+1}) - h_u \hat{s}_{iz} - (-1)^i h_s \hat{s}_{ix}, \quad (26)$$

which includes the effective uniform field h_u and the induced staggered field $h_s \propto h_u$ perpendicular to both the applied uniform magnetic field and the Dzyaloshinsky vector.

4.2. Staggered external field

Application of a staggered field $\mathbf{h}^V$ for an antiferromagnetically coupled Cu_1–Cu_2 pair produces a local spin polarization on both copper and oxygen sites,

$$\langle \mathbf{S}_i \rangle = \frac{1}{J^2_{12}} [\mathbf{D}^{(i)}_{12} \times \mathbf{h}^V] = \overleftrightarrow{\chi}^{SV}(i) \mathbf{h}^V, \quad (27)$$

which can be detected by different site-sensitive methods including neutron diffraction and, mainly, by nuclear magnetic resonance. We note that the SV-susceptibility tensor is antisymmetric:

$$\chi^{SV}_{\alpha\beta} = -\chi^{SV}_{\beta\alpha}.$$

Strictly speaking, both formulas (25) and (27) work well only in the paramagnetic regime and for relatively weak external fields.

Above, we addressed a single Cu_1–O–Cu_2 bond, where, despite the site location, the direction and magnitude of the Dzyaloshinsky vector depend strongly on the bond strength and geometry. It is clear that a site rather than a bond location of DM vectors require revisiting conventional symmetry considerations and the magnetic structure in weak ferro- and antiferromagnets. Interestingly, expression (27) predicts the effects of a constructive or destructive (frustration) interference of copper spin polarizations in one-, two-, and three-dimensional lattices depending on the relative sign of Dzyaloshinsky vectors and staggered fields for nearest neighbors. We note that with the destructive interference, the local copper spin polarization may vanish, with the DM coupling then manifesting itself only through the oxygen spin polarization. Another interesting manifestation of the oxygen DM antisymmetric exchange coupling concerns the edge-shared CuO_2 chains (see Fig. 2), ubiquitous for many cuprates, where we deal with an exact compensation of copper contributions to Dzyaloshinsky vectors and the unique possibility to observe the effects of uncompensated but oppositely directed local oxygen contributions. It is worth noting that for purely antiferromagnetic in-chain ordering, the oxygen spin polarization induced due to the d–p-covalency by two neighboring Cu ions is in fact compensated. In other words, the oxygen ions are expected to be nonmagnetic. However, the situation changes if a nonzero oxygen DM coupling is taken into account. Indeed, applying the staggered field, for instance, along

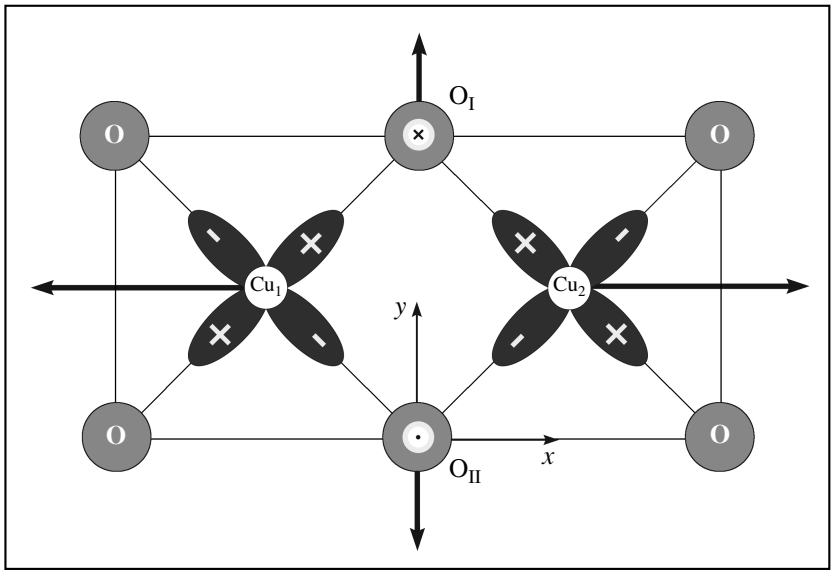

Fig. 2. The fragment of a typical edge-shared CuO_2 chain with copper and oxygen spin orientation under a staggered field applied along the x-direction. Note the antiparallel orientation of oxygen Dzyaloshinsky vectors

the chain direction (O_x) we arrive in accordance with Eq. (27) at a staggered spin polarization of oxygen ions in an orthogonal O_y direction, whose magnitude is expected to be strongly enhanced due to the usually small magnitudes of a 90°-symmetric superexchange. In general, the direction of the oxygen staggered spin polarization is to be perpendicular to both the main chain antiferromagnetic vector and the CuO_2 chain normal.

We emphasize that the net in-chain Dzyaloshinsky vector

$$\mathbf{D} = \mathbf{D}^{(1)} + \mathbf{D}^{(O_I)} + \mathbf{D}^{(O_{II})} + \mathbf{D}^{(2)}$$

vanishes, and hence, in terms of the conventional approach to the DM theory, we miss the anomalous oxygen spin polarization effect. In this connection, it is worth noting the neutron diffraction data in [27], which unambiguously evidence the oxygen momentum formation and canting in edge-shared CuO_2 chain cuprate Li_2CuO_2. Anyhow, we predict an interesting possibility to find a purely oxygen contribution to the DM coupling.

5. ^{17}O NMR AS AN EFFECTIVE TOOL TO INSPECT DM COUPLING FOR Cu–O–Cu BONDS

The ligand nuclear magnetic resonance appears to be an effective tool for inspecting all the peculiarities of the DM coupling in weak ferromagnets. This possibility was illustrated earlier with ^{19}F NMR for weak ferromagnet FeF_3 [26]. The remarkable progress in the ^{17}O NMR–NQR investigations as a spin-off of the cuprate activity provides unique opportunities to elucidate subtle details of the electron and spin structure for both parent and doped cuprates with the DM coupling.

Detailed study of the ligand ^{17}O hyperfine couplings in weak ferromagnetic La_2CuO_4 for temperatures ranging from 285 to 800 K undertaken in [13] has uncovered puzzling anomalies of the ^{17}O Knight shift. The authors made the surprising conclusion that in approaching T_N, the planar oxygen hyperfine tensor a) reverses its sign, b) becomes enhanced by much more than an order of magnitude, and c) exhibits 100 % anisotropy. The anomalously large negative ^{17}O Knight shift was observed only when external field was parallel to the local Cu–O–Cu bond axis (PL1 lines [13]) or perpendicular to the CuO_2 plane. The effect was not observed for the NMR signal corresponding to oxygen in the local Cu–O–Cu bonds whose axis is perpendicular to the in-plane external field (PL2 lines [13]). In their opinion, these characteristics do not correspond to any known hyperfine mechanism, but are somewhat reminiscent of the functional form of the DM exchange coupling. Such an effect has not yet been reported for any other system. It is worth noting once more that experimental data were mainly collected in a paramagnetic state for temperatures well above T_N, where there are no frozen

moments! The data were first interpreted as an indication of a direct oxygen spin polarization due to a local DM antisymmetric exchange coupling. However, this requires unphysically large values for such a polarization, and hence the dramatic ^{17}O hyperfine tensor anomaly remains unexplained up to now [13].

5.1. ^{17}O–Cu transferred hyperfine interactions: ferro- and antiferromagnetic terms

Our interpretation of ligand NMR data in low-symmetry systems such as La_2CuO_4 implies a thorough analysis of both spin canting effects and transferred hyperfine interactions; we revisit some textbook results that are standard for model high-symmetry systems. We start with the spin–dipole hyperfine interactions for O $2p$-holes, which are main participants of Cu_1–O–Cu_2 bonding. Using the conventional formula for a spin–dipole contribution to the local field,

$$\mathcal{H}_n = -g_s\mu_B \sum_i \frac{3(\mathbf{r}_i\cdot\mathbf{s}_i)\mathbf{r}_i - r_i^2\mathbf{s}_i}{r_i^5},$$

and calculating the appropriate matrix elements on oxygen $2p$-functions as

$$\left\langle p_i \left| \frac{3x_\alpha x_\beta - r^2\delta_{\alpha\beta}}{r^5} \right| p_j \right\rangle = -\frac{2}{5}\left\langle \frac{1}{r^3}\right\rangle_{2p} \langle p_i|3\widetilde{l_\alpha l_\beta} - 2\delta_{\alpha\beta}|p_j\rangle = \frac{2}{5}\left\langle \frac{1}{r^3}\right\rangle_{2p}\left(\frac{3}{2}\delta_{\alpha i}\delta_{\beta j} + \frac{3}{2}\delta_{\alpha j}\delta_{\beta i} - \delta_{\alpha\beta}\delta_{ij}\right), \quad (28)$$

we represent the local field on the ^{17}O nucleus in the Cu_1–O–Cu_2 system as a sum of ferro- and antiferromagnetic contributions [26]:

$$\mathcal{H}_n = \overleftrightarrow{\mathbf{A}}^S \cdot \langle\hat{\mathbf{S}}\rangle + \overleftrightarrow{\mathbf{A}}^V \cdot \langle\hat{\mathbf{V}}\rangle, \quad (29)$$

where

$$\overleftrightarrow{\mathbf{A}}^S = \overleftrightarrow{\mathbf{A}}^S(dp) + \overleftrightarrow{\mathbf{A}}^S(pd), \quad \overleftrightarrow{\mathbf{A}}^V = \overleftrightarrow{\mathbf{A}}^V(pd) - \overleftrightarrow{\mathbf{A}}^V(dp),$$

$$A^S_{ij}(dp) = A^{(0)}_p[3c_t(dp_i)c_t(dp_j) - |\mathbf{c}_t(dp)|^2\delta_{ij}],$$

$$A^S_{ij}(pd) = A^{(0)}_p[3c_t(p_id)c_t(p_jd) - |\mathbf{c}_t(pd)|^2\delta_{ij}],$$

$$A^V_{ij}(dp) = A^{(0)}_p[3c_s(\widetilde{dp_i)c_t}(dp_j) - (\mathbf{c}_s(dp)\cdot\mathbf{c}_t(dp))\delta_{ij}],$$

$$A^V_{ij}(pd) = A^{(0)}_p[3c_s(\widetilde{p_id)c_t}(p_jd) - (\mathbf{c}_s(pd)\cdot\mathbf{c}_t(pd))\delta_{ij}],$$

where

$$A^{(0)}_p = \frac{2}{5}g_s\mu_B\left\langle\frac{1}{r^3}\right\rangle_{2p}$$

and the tilde denotes symmetrization. Thus, along with the conventional textbook ferromagnetic ($\propto\langle\hat{\mathbf{S}}\rangle$) transferred hyperfine contribution to the local field, which simply mirrors the sum of two Cu–O bonds, we arrive at an additional unconventional difference ($\propto\langle\hat{\mathbf{V}}\rangle$), or staggered (antiferromagnetic) contribution whose symmetry and magnitude strongly depend on the orientation of the oxygen crystal field axes and the Cu_1–O–Cu_2 bonding angle. In the case of the Cu_1–O–Cu_2 geometry shown in Fig. 1, we arrive at a diagonal $\overleftrightarrow{\mathbf{A}}^S$ tensor:

$$A^S_{xx} = 2A_p\left(3\sin^2\frac{\theta}{2} - 1\right),$$

$$A^S_{yy} = 2A_p\left(3\cos^2\frac{\theta}{2} - 1\right),$$

$$A^S_{zz} = -2A_p, \quad (30)$$

and the only nonzero xy, yx-components of the $\overleftrightarrow{\mathbf{A}}^V$ tensor are

$$A^V_{xy} = A^V_{yx} = 3A_p\sin\theta, \quad (31)$$

with

$$A_p = \frac{3}{4}\left(\frac{t_{dp\sigma}}{\epsilon_p}\right)^2 A^0_p = f_\sigma A^0_p, \quad (32)$$

where f_σ is the parameter of a transferred spin density and we use the simple approximation $E_{s,t}(dp_{x,y}) \approx \epsilon_p$[3)]. Thus, the ligand ^{17}O NMR provides an effective tool to inspect the spin canting effects in oxides with the DM coupling in both paramagnetic and ordered phases.

5.2. Anomalous ^{17}O Knight shift in La_2CuO_4 as a manifestation of the field-induced staggered spin polarization

The two-term structure of the oxygen local field implies a two-term SV-structure of the ^{17}O Knight shift

$$^{17}K = \overleftrightarrow{\mathbf{A}}^S\overleftrightarrow{\chi}^{SS} + \overleftrightarrow{\mathbf{A}}^V\overleftrightarrow{\chi}^{VS}, \quad (33)$$

which points to the Knight shift as an effective tool to inspect both uniform and staggered spin polarization. The existence of an antiferromagnetic term in oxygen hyperfine interactions yields a rather simple explanation of the ^{17}O Knight shift anomalies in La_2CuO_4 [13]

[3)] Generally speaking, we should take an additional contribution of magneto-dipole hyperfine interactions into account.

as a result of the external-field-induced staggered spin polarization

$$\langle\hat{\mathbf{V}}\rangle = \mathbf{L} = \overset{\leftrightarrow}{\chi}^{VS}\mathcal{H}_{ext}.$$

Indeed, "our" local y axis for the Cu_1–O–Cu_2 bond corresponds to the crystal tetragonal c axis oriented perpendicular to CuO_2 planes in both LTO and LTT phases of La_2CuO_4, while the x axis corresponds to the local Cu–O–Cu bond axis. This means that for the geometry of the experiment in [13] (with the crystal oriented such that the external uniform field was either parallel or perpendicular to the local Cu–O–Cu bond axis), the antiferromagnetic contribution to the ^{17}O Knight shift is observed only a) for oxygen in Cu_1–O–Cu_2 bonds oriented along the external field or b) for the external field along the tetragonal c axis. Experimental data in [13] agree with the staggered magnetization along the tetragonal c axis in case a) and along the rhombic c axis (tetragonal ab axis) in case b). With $L = 1$, $A_p^{(0)} \approx +100$ kG/spin (see Ref. [13]), $|\sin\theta| \approx 0.1$, and $f_\sigma \approx 20\,\%$, we obtain ≈ 6 kG as the maximum value of the low-temperature antiferromagnetic contribution to the hyperfine field, which is equivalent to a giant ^{17}O Knight shift of the order of almost 10 %. Nevertheless, this value agrees with a low-temperature extrapolation of the high-temperature experimental data in [13]. Interestingly, a sizeable effect of the anomalous negative contribution to the ^{17}O Knight shift has been observed in La_2CuO_4 well inside the paramagnetic state for temperatures $T \approx 500$ K, essentially higher than $T_N \approx 300$ K. This points to a close relation between the magnitude of the field-induced staggered magnetization and the spin-correlation length, which increases as T_N is approached.

The ferro-antiferromagnetic SV-structure of the local field on the nucleus of an intermediate oxygen ion in a Cu_1–O–Cu_2 triad points to ^{17}O NMR as, probably, the only experimental technique to measure the value and direction of the Dzyaloshinsky vector. For instance, the negative sign of the ^{17}O Knight shift in La_2CuO_4 [13] points to a negative sign of $\overset{\leftrightarrow}{\chi}^{VS}$ for the Cu_1–O–Cu_2 triad with $A^V_{xy} > 0$, and hence to a positive sing of the z-component of the net Dzyaloshinsky vector in the Cu_1–O–Cu_2 triad with the geometry shown in Fig. 1 for $\theta \le \pi$, $\delta_1 = \delta_2 \approx \pi/2$. We emphasize that the above effect is determined by the net Dzyaloshinsky vector in the Cu_1–O–Cu_2 triad rather than by a local oxygen "weak-ferromagnetic" polarization as was first proposed in [13]

A similar effect of the anomalous ligand ^{13}C Knight shift was recently observed in copper pyrimidine dinitrate $[CuPM(NO_3)_2(H_2O)_2]_n$, a one-dimensional $S = 1/2$ antiferromagnet with the alternating local symmetry, and was also interpreted in terms of the field-induced staggered magnetization [28]. However, the authors took only the inter-site magneto-dipole contribution to the $\overset{\leftrightarrow}{\mathbf{A}}^{V}$ tensor into account, which questions their quantitative conclusions regarding the "giant" spin canting in CuO_2 chains.

6. SYMMETRIC SPIN ANISOTROPY

The symmetric two-ion spin anisotropy ia a symmetric partner of the DM coupling; both are usually addressed on equal footing as two main exchange-relativistic interactions. The symmetric spin anisotropy for a Cu_1–Cu_2 pair is described by the effective Hamiltonian

$$\hat{H}_{an} = \frac{1}{4}\hat{\mathbf{S}}\overset{\leftrightarrow}{\mathbf{K}}^{S}\hat{\mathbf{S}} - \frac{1}{4}\hat{\mathbf{V}}\overset{\leftrightarrow}{\mathbf{K}}^{V}\hat{\mathbf{V}} \qquad (34)$$

with kinematic relations (7). Depending on the sign of the anisotropy constants, we arrive at two types of spin configurations minimizing the energy of spin anisotropy: the conventional twofold-degenerate ferromagnetic state or an unconventional multiple-degenerate antiferromagnetic state. As a relevant illustrative example, we refer to the axial anisotropy

$$\hat{H}_{an} = K\hat{S}_z^2,$$

which stabilizes the $|1 \pm 1\rangle$ doublet for $K < 0$ or a set of superposition states

$$\Psi_{\alpha,\phi} = \cos\alpha|00\rangle + e^{i\phi}\sin\alpha|10\rangle \qquad (35)$$

for $K > 0$. The latter incorporates the limiting configurations $|00\rangle$ and $|10\rangle$, the Néel doublet

$$\frac{1}{\sqrt{2}}(|00\rangle \pm |10\rangle),$$

the Dzyaloshinsky–Moriya doublet

$$\frac{1}{\sqrt{2}}(|00\rangle \pm i|10\rangle),$$

and their arbitrary superpositions.

As usual, the term is processed using a number of simple model approximations. First, instead of the generalized form in (34), we consider a pseudodipole anisotropy

$$\hat{H}_{an} = \hat{\mathbf{s}}_1\overset{\leftrightarrow}{\mathbf{K}}_{12}\hat{\mathbf{s}}_2\,. \qquad (36)$$

Second, we use a trivial local mean-field-approximation (MFA) approach, whose applicability for $s = 1/2$ spin systems is questionable. Indeed, calculating the classical energy of the pseudodipole two-ion anisotropy

$$K\langle \hat{s}_{1z}\rangle\langle \hat{s}_{2z}\rangle = \frac{1}{4}K(\langle \hat{S}_z\rangle^2 - \langle \hat{V}_z\rangle^2)$$

and the respective quantum energy

$$K\langle \hat{s}_{1z}\hat{s}_{2z}\rangle = \frac{1}{4}K(\langle \hat{S}_z^2\rangle - \langle \hat{V}_z^2\rangle)$$

for the two-ion state

$$\Psi_{\alpha,0} = \cos\alpha|00\rangle + \sin\alpha|1n\rangle$$

induced by a Néel-like staggered field $\mathbf{h}^V \parallel \mathbf{n}$, we obtain

$$E_{class} = -\frac{1}{4}K\sin 2\alpha \cdot n_z^2,$$

$$E_{quant} = \frac{1}{4}K(1 - 2\sin^2\alpha \cdot n_z^2),$$

which evidences the crucial importance of quantum effects when addressing the numerical aspect of spin anisotropy. We note that the mean value $\langle \hat{V}_z^2\rangle$ reaches the maximum ($= 1$) on a set of superposition states (35), while $\langle \hat{V}_z\rangle^2$ does on a single Néel state $\Psi_{\alpha=\pi/4,\phi=0}$.

6.1. Effective symmetric spin anisotropy due to the DM interaction

Speaking about an effective spin anisotropy due to the DM interaction, one usually addresses a simple classical two-sublattice weak ferromagnet where the free energy has a minimum when both ferro- ($\propto \langle \hat{\mathbf{S}}\rangle$) and antiferromagnetic ($\propto \langle \hat{\mathbf{V}}\rangle$) vectors, being perpendicular to each other, lie in the plane perpendicular to the Dzyaloshinsky vector $\mathbf{D}$. However, the issue is rather involved and appeared to be hotly debated for a long time [9, 10, 29, 30]. In our opinion, we should first of all define what the spin anisotropy is. Indeed, the description of any spin system implies that the free energy Φ depends on a set of vectorial order parameters (e.g., $\langle \hat{\mathbf{S}}\rangle, \propto \langle \hat{\mathbf{V}}\rangle, \propto \langle \hat{\mathbf{T}}\rangle$) under a kinematic constraint, rather than a single magnetic moment as in a simple ferromagnet, which can make the orientational dependence of Φ extremely complicated. Such a situation requires a careful analysis of the corresponding spin Hamiltonian with a choice of proper approximations.

The effective symmetric spin anisotropy due to the DM interaction can be easily derived as a second-order perturbation correction due to the DM coupling as

$$\hat{H}_{an}^{DM} = \hat{P}\hat{H}_{DM}\hat{R}\hat{H}_{DM}\hat{P},$$

where $\hat{P}$ is the projection operator projecting on the ground manifold and

$$\hat{R} = \frac{1 - \hat{P}}{E_0 - \hat{H}_0}.$$

For an antiferromagnetically coupled spin-1/2 pair, $\hat{H}_{an}^{DM}$ can be written as

$$\hat{H}_{an}^{DM} = \sum_{i,j}\Delta K_{ij}^V \hat{V}_i\hat{V}_j$$

with

$$\Delta K_{ij}^V = \frac{1}{8J}D_iD_j$$

if $|\mathbf{D}| \ll J$. We thus see that in the framework of the simple MFA approach, this anisotropy stabilizes a Néel state with $\langle \hat{\mathbf{V}}\rangle \perp \mathbf{D}$. But this is actually an MFA artefact. Indeed, we examine the second-order perturbation correction to the ground state energy of an antiferromagnetically coupled spin-1/2 pair in a Néel-like staggered field $\mathbf{h}^V \parallel \mathbf{n}$,

$$E_{an}^{DM} = -\frac{|\mathbf{D}\cdot\mathbf{n}|^2}{4(E_\parallel - E_g)} - \frac{|\mathbf{D}\times\mathbf{n}|^2}{4(E_\perp - E_g)}\cos^2\alpha, \qquad (37)$$

where

$$E_\perp = J, \quad E_\parallel = J\cos^2\alpha + h^V\sin 2\alpha,$$

$$E_g = J\sin^2\alpha - h^V\sin 2\alpha.$$

The first term in (37) stabilizes the $\mathbf{n} \parallel \mathbf{D}$ configuration and the second stabilizes the $\mathbf{n} \perp \mathbf{D}$ configuration. Interestingly,

$$(E_\parallel - E_g)\cos^2\alpha = E_\perp - E_g,$$

that is, for any staggered field, E_{an}^{DM} is independent of its orientation, because

$$|\mathbf{D}\cdot\mathbf{n}|^2 + |\mathbf{D}\times\mathbf{n}|^2 = |\mathbf{D}|^2.$$

In other words, at variance with the simple MFA approach, the DM contribution to the energy of anisotropy for an exchange-coupled spin-1/2 pair in a staggered field vanishes. The conclusion proves to be correct in the limit of a zero field as well.

6.2. Microscopics of symmetric spin anisotropy

Anyway, the $\hat{H}_{an}^{DM}$ term has not to be included into effective spin anisotropy Hamiltonian (6). As regards the true symmetric two-ion spin anisotropy (pseudodipole, or exchange anisotropy), its magnitude can be obtained if all other effects quadratic in the spin–orbital coupling are taken into account. At variance with the effective DM spin Hamiltonian, the symmetric spin anisotropy evolves from the higher-order perturbation effects, which makes its analysis even more involved and can lead to many misleading estimations. Similarly to the case of the DM interaction, we deal with two competing contributions. The first is derived as the lowest-order contribution that does not take account of orbital fluctuations for $Cu_{1,2}$ $3d$ states. For this, we consider the effects of spin–orbital mixing for the ground-state singlet and triplet 101 configurations perturbed by covalent effects. Assuming the validity of the conventional perturbation series, we arrive at a modified expression for the corresponding functions as

$$\Psi_{101;SM} = \Phi_{101;SM} + \sum_{\{n\}\Gamma} c_{\{n\}}(^{2S+1}\Gamma) \left[\Phi_{\{n\};\Gamma SM} - \sum_{S'M'\Gamma'} \frac{\langle \{n\};\Gamma' S'M'|V_{so}|\{n\};\Gamma SM\rangle}{E_{^{2S'+1}\Gamma'}(\{n\}) - E_{^{2S+1}\Gamma_0}(101)} \Phi_{\{n\};\Gamma' S'M'} \right] \tag{38}$$

and then obtain the expressions for the tensorial anisotropy parameters (see Eq. (13)):

$$K_{ij}^{S} = \sum_{\{n\}\Gamma_1,\Gamma_2,\Gamma'} c_{\{n\}}^{*}(^3\Gamma_1) c_{\{n\}}(^3\Gamma_2) \frac{\langle \{n\};^3\Gamma_1|\Lambda_i^S|\{n\};^3\Gamma'\rangle\langle \{n\};^3\Gamma'|\Lambda_j^S|\{n\};^3\Gamma_2\rangle}{E_{^3\Gamma'}(\{n\}) - E_{^3\Gamma_0}(101)}, \tag{39}$$

$$K_{ij}^{V} = \sum_{\{n\}\Gamma_1,\Gamma_2,\Gamma'} c_{\{n\}}^{*}(^3\Gamma_1) c_{\{n\}}(^3\Gamma_2) \frac{\langle \{n\};^3\Gamma_1|\Lambda_i^V|\{n\};^1\Gamma'\rangle\langle \{n\};^1\Gamma'|\Lambda_j^V|\{n\};^3\Gamma_2\rangle}{E_{^1\Gamma'}(\{n\}) - E_{^3\Gamma_0}(101)}. \tag{40}$$

It follows that K_{ij}^S and K_{ij}^V are determined by the triplet–triplet and singlet–triplet mixing, respectively. Interestingly, for nonzero orbital matrix elements in (39) and (40), we find

$$\langle \{n\};^3\Gamma_1|\Lambda_i^S|\{n\};^3\Gamma'\rangle = \langle \{n\};^3\Gamma_1|\Lambda_i^V|\{n\};^1\Gamma'\rangle,$$

and hence

$$K_{ij}^S = K_{ij}^V$$

if we suppose that

$$E_{^1\Gamma'}(\{n\}) = E_{^3\Gamma'}(\{n\}),$$

which is equivivalent to neglecting the singlet–triplet splitting for Γ' terms, or the respective exchange effects. We note that the contribution of the two-hole one-site 200, 002, and 020 configurations in (39) and (40) is actually related to an one-site, or single-ion spin anisotropy. Thus, we conclude that, strictly speaking, a simple two-site pseudodipole form of symmetric anisotropy (1) fails to correctly capture all the features of spin anisotropy in our three-center two-hole system. This primarily concerns the quantitative predictions and estimations. The contribution the two-hole two-site 110 and 011 configurations to spin anisotropy turns out to be nonzero only if the p–d-exchange is taken into account.

The second contribution is associated with orbital fluctuations for $Cu_{1,2}$ $3d$ states within the ground-state 101 configuration and evolves from a third-order combined effect of $Cu_{1,2}$ spin–orbital $V_{so}(Cu_{1,2})$ and effective Cu_1–Cu_2 exchange couplings (see, e.g., a detailed analysis of similar terms in Ref. [31]). It is worth noting that following [32], just this contribution is usually considered to be the only source of the effective pseudodipole anisotropy for Cu_1–O–Cu_2 triads in cuprates (see, e.g., Ref. [33]). Thus, we see that any decisive conclusions regarding the quantitative estimations of symmetric spin anisotropy imply a thorough analysis of the numerous competing contributions that were classified above.

7. CONCLUSIONS

We have revisited and generalized the conventional Moriya approach to the antisymmetric exchange coupling in cuprates specifying the local spin–orbital contributions to the Dzyaloshinsky vector focusing on the oxygen term. We have applied a scheme that provides an optimal way to account for intra-atomic electron correlations and low-symmetry crystal field, and

to separate the local contributions to the Dzyaloshinsky vector. The Dzyaloshinsky vector and the corresponding weak ferromagnetic momentum are shown to be a superposition of comparable and, sometimes, competing local Cu and O contributions. In this connection, it is worth noting that the anyonic contribution to the Dzyaloshinsky vector is crucial for the very existence of the DM coupling in the pair of rare-earth ions (e.g., Yb^{3+}–As^{4-}–Yb^{3+} triads in Yb_4As_3 [34]) because a very strong spin–orbital coupling for rare-earth ions is diagonalized within a ground state multiplet.

We have shown that the staggered magnetic field $\mathbf{h}^V$ applied to edge-shared CuO_2 chains induces the oxygen staggered spin polarization in the direction $\propto [\mathbf{h}^V \times \mathbf{m}]$ (where $\mathbf{m}$ is a vector perpendicular to the CuO_2 plane) due to uncompensated oxygen Dzyaloshinsky vectors. Its experimental observation could provide a direct evidence of the oxygen DM coupling. The intermediate ^{17}O NMR is shown to be an effective tool for inspecting the effects of Dzyaloshinsky–Moriya coupling in an external magnetic field. The anisotropic antiferromagnetic contribution to ^{17}K explains the puzzling anomalies observed in La_2CuO_4 [13]. We have revisited the effects of symmetric spin anisotropy, in particular, those directly induced by the Dzyaloshinsky–Moriya coupling. The perturbation scheme that we applied generalizes the well-known Moriya approach and presents a basis for reliable quantitative estimations of the symmetric partner of the Dzyaloshinsky–Moriya coupling. At variance with the conventional standpoint, the parameters of the effective two-ion spin anisotropy are shown to incorporate contributions of a single-ion anisotropy for two-hole configurations on both the Cu and O sites.

I thank R. Walstedt for the stimulating and encouraging discussion, and H. Eschrig, M. Richter, and S.-L. Drechsler for their interest and the useful discussion. I thank Leibniz-Institut für Festkörper- und Werkstoffforschung Dresden, where part of this work was done, for hospitality. This work is supported in part by the CRDF (grant № REC-005) and RFBR (grants №№ 04-02-96077, 06-02-17242, and 06-03-90893).

REFERENCES

1. A. S. Borovik-Romanov and M. P. Orlova, Sov. Phys. JETP **4**, 531 (1957).

2. I. E. Dzialoshinskii, Sov. Phys. JETP **5**, 1259 (1957); I. E. Dzyaloshinskii, J. Phys. Chem. Sol. **4**, 241 (1958).

3. T. Moriya, Phys. Rev. Lett. **4**, 228 (1960); Phys. Rev. **120**, 91 (1960).

4. A. S. Moskvin and I. G. Bostrem, Fiz. Tverd. Tela **19**, 2616 (1977).

5. T. Thio, T. R. Thurster, N. W. Preyer, P. J. Picone, M. A. Kastner, H. P. Jenssen, D. R. Gabbe, C. Y. Chen, R. J. Birgeneau, and A. Aharony, Phys. Rev. B **38**, 905 (1988).

6. M. Oshikawa and I. Affleck, Phys. Rev. Lett. **79**, 2883 (1997); I. Affleck and M. Oshikawa, Phys. Rev. B **60**, 1038 (1999).

7. D. Coffey, T. M. Rice, and F. C. Zhang, Phys. Rev. B **44**, 10112 (1991); N. E. Bonesteel, T. M. Rice, and F. C. Zhang, Phys. Rev. Lett. **68**, 26844 (1992); N. E. Bonesteel, Phys. Rev. B **47**, 11302 (1993).

8. W. Koshibae, Y. Ohta, and S. Maekawa, Phys. Rev. B **47**, 3391 (1993); Phys. Rev. B **50**, 3767 (1994).

9. L. Shekhtman, O. Entin-Wohlman, and A. Aharony, Phys. Rev. Lett. **69**, 836 (1992).

10. W. Koshibae, Y. Ohta, and S. Maekawa, Phys. Rev. Lett. **71**, 467 (1993); L. Shekhtman, O. Entin-Wohlman, and A. Aharony, Phys. Rev. Lett. **71**, 468 (1993).

11. I. Tsukada, X. F. Sun, S. Komiya, A. N. Lavrov, and Y. Ando, Phys. Rev. B **67**, 224401 (2003).

12. M. Hücker, V. Kataev, J. Pommer, U. Ammerahl, A. Revcolevschi, J. M. Tranquada, and B. Büchner, Phys. Rev. B **70**, 214515 (2004).

13. R. E. Walstedt, B. S. Shastry, and S. W. Cheong, Phys. Rev. Lett. **72**, 3610 (1994); R. E. Walstedt and S. W. Cheong, Phys. Rev. B **64**, 014404 (2001).

14. A. Kolezhuk and T. Vekua, Phys. Rev. B **72**, 094424 (2005).

15. T. Rõõm, D. Hüvonen, U. Nagel, J. Hwang, T. Timusk, and H. Kageyama, Phys. Rev. B **70**, 144417 (2004).

16. P. W. Anderson, Phys. Rev. **115**, 2 (1959); Sol. St. Phys. **14**, 99 (1963).

17. L. Shekhtman, A. Aharony, and O. Entin-Wohlman, Phys. Rev. B **47**, 174 (1993).

18. W. Low, *Paramagnetic Resonance in Solids*, in *Solid State Physics*, Suppl. II, Acad. Press, N.Y., London (1960).

19. T. Yildirim, A. B. Harris, O. Entin-Wohlman, and A. Aharony, Phys. Rev. Lett. **73**, 2919 (1994); T. Yildirim, A. B. Harris, A. Aharony, and O. Entin-Wohlman, Phys. Rev. B **52**, 10239 (1995).

20. S. Tornow, O. Entin-Wohlman, and A. Aharony, Phys. Rev. B **60**, 10206 (1999).

21. G. Herzberg, Proc. Roy. Soc. (London) Ser. A **248**, 309 (1958); L. Veseth, J. Phys. B: Atom. Mol. Phys. **16**, 2713 (1983).

22. S. Renold, S. Pliberŝek, E. P. Stoll, T. A. Claxton, and P. F. Meier, Eur. Phys. J. B **23**, 3 (2001).

23. F. Keffer, Phys. Rev. **126**, 896 (1962).

24. H. Eskes and G. A. Sawatzky, Phys. Rev. B **43**, 119 (1991).

25. A. S. Moskvin, R. Neudert, M. Knupfer, J. Fink, and R. Hayn, Phys. Rev. B **65**, 180512(R) (2002).

26. A. S. Moskvin, Sov. Phys. Sol. St. **32**, 959 (1990).

27. E. M. L. Chung, G. J. McIntyre, D. McK. Paul, G. Balakrishnan, and M. R. Lees, Phys. Rev. B **68**, 144410 (2003).

28. A. U. B. Wolter, P. Wzietek, S. Sullow, F. J. Litterst, A. Honecker, W. Brenig, R. Feyerherm, and H.-H. Klauss, Phys. Rev. Lett. **94**, 057204 (2005).

29. A. Zheludev, S. Maslov, G. Shirane, I. Tsukada, T. Masuda, K. Uchinokura, I. A. Zaliznyak, R. Erwin, and L. P. Regnault, Phys. Rev. B **59**, 11432 (1999).

30. M. D. Lumsden, B. C. Sales, D. Mandrus, S. E. Nagler, and J. R. Thompson, Phys. Rev. Lett. **86**, 159 (2001).

31. A. S. Moskvin, I. G. Bostrem, and M. A. Sidorov, Zh. Eksp. Teor. Fiz. **103**, 2499 (1993).

32. K. Yosida, J. Appl. Phys. **39**, 511 (1960).

33. V. Y. Yushankhai and R. Hayn, Europhys. Lett. **47**, 116 (1999).

34. M. Oshikawa, K. Ueda, H. Aoki, A. Ochiai, and M. Kohgi, J. Phys. Soc. Jpn. **68**, 3181 (1999).